AGU PUBLICATIONS
JGR
Journal of Geophysical Research: Space Physics

RESEARCH ARTICLE
10.1002/2014JA020630

Key Points:
- Critical assessment of the TEC from Mars Express MARSIS instrument
- TEC from subsurface algorithms and active ionospheric sounding comparison
- MARSIS data sets evaluation by NeMars empirical model

Correspondence to:
B. Sánchez-Cano,
bscmdr1@leicester.ac.uk

Citation:
Sánchez-Cano, B., et al. (2015), Total electron content in the Martian atmosphere: A critical assessment of the Mars Express MARSIS data sets, *J. Geophys. Res. Space Physics*, *120*, 2166–2182, doi:10.1002/2014JA020630.

Received 17 SEP 2014
Accepted 29 JAN 2015
Accepted article online 4 FEB 2015
Published online 9 MAR 2015

Total electron content in the Martian atmosphere: A critical assessment of the Mars Express MARSIS data sets

B. Sánchez-Cano[1,2], D. D. Morgan[3], O. Witasse[4], S. M. Radicella[5], M. Herraiz[2,6], R. Orosei[7], M. Cartacci[8], A. Cicchetti[8], R. Noschese[8], W. Kofman[9,10], C. Grima[11], J. Mouginot[12], D. A. Gurnett[3], M. Lester[1], P.-L. Blelly[13], H. Opgenoorth[14], and G. Quinsac[4]

[1]Radio and Space Plasma Physics Group, Department of Physics and Astronomy, University of Leicester, Leicester, UK, [2]Facultad de Ciencias Físicas, Departamento de Física de la Tierra, Astronomía y Astrofísica I, Universidad Complutense de Madrid, Madrid, Spain, [3]Department of Physics and Astronomy, University of Iowa, Iowa City, Iowa, USA, [4]ESTEC–Scientific Support Office, European Space Agency, Noordwijk, Netherlands, [5]Telecommunications/ICT for Development Laboratory, Abdus Salam International Centre for Theoretical Physics, Trieste, Italy, [6]Instituto de Geociencias (UCM, CSIC), Madrid, Spain, [7]Istituto di Radioastronomia, Istituto Nazionale di Astrofisica, Bologna, Italy, [8]Istituto di Astrofisica e Planetologia Spaziali, Istituto Nazionale di Astrofisica, Rome, Italy, [9]UJF-Grenoble1/CNRS-INSU, Institut de Planétologie et d'Astrophysique de Grenoble UMR 5274, Grenoble, France, [10]Visiting Professor at Space Research Centre, Polish Academy of Sciences, Warsaw, Poland, [11]Institute for Geophysics, University of Texas, Austin, Texas, USA, [12]Department of Earth System Science, University of California, Irvine, California, USA, [13]Institut de Recherche en Astrophysique et Planétologie, Toulouse, France, [14]Swedish Institute of Space Physics, Uppsala Division, Uppsala, Sweden

Abstract The total electron content (TEC) is one of the most useful parameters to evaluate the behavior of the Martian ionosphere because it contains information on the total amount of free electrons, the main component of the Martian ionospheric plasma. The Mars Express Mars Advanced Radar for Subsurface and Ionosphere Sounding (MARSIS) radar is able to derive TEC from both of its operation modes: (1) the active ionospheric sounding (AIS) mode and (2) the subsurface mode. TEC estimates from the subsurface sounding mode can be computed from the same raw data independently using different algorithms, which should yield similar results. Significant differences on the dayside, however, have been found from two of the algorithms. Moreover, both algorithms seem also to disagree with the TEC results from the AIS mode. This paper gives a critical, quantitative, and independent assessment of these discrepancies and indicates the possible uncertainty of these databases. In addition, a comparison between the results given by the empirical model of the Martian ionosphere developed by Sánchez-Cano et al. (2013) and the different data sets has been performed. The main result is that for solar zenith angles higher than 75°, where the maximum plasma frequency is typically small compared with the radar frequencies, the two subsurface algorithms can be confidently used. For solar zenith angles less than 75°, where the maximum plasma frequency is very close to the radar frequencies, both algorithms suffer limitations. Nevertheless, despite the solar zenith angle restrictions, the dayside TEC of one of the two algorithms is consistent with the modeled TEC.

1. Introduction

The total electron content (TEC) in the atmosphere is defined as the number of free electrons contained in a column with the cross section of 1 m^2 along a vertical propagation path from the planetary surface to a point above the atmosphere. This relation is expressed as the integral of the electron density along a path in the ionosphere, given by

$$\mathrm{TEC} = \int_{h_i}^{h_f} Ne \ \mathrm{dh} \quad (1)$$

where h_i and h_f are the initial and final points of the path, respectively. If the objective was to obtain the TEC of the whole electron content in the atmosphere, in the ideal case, h_i would correspond to 0 km and h_f to infinity. The units of TEC are electrons per square meter, and conventionally, 10^{16} el/m^2 is defined as 1 total electron content unit (TECu), 1 TECu = 10^{16} el/m^2. On Earth, typical vertical TEC values range between 10^{17} and 10^{18} el/m^2 [*Hargreaves*, 1992] or 10–100 TECu. Earth TEC varies with geomagnetic location, local time, season, solar EUV flux, and magnetic activity. TEC values for the ionosphere of Mars are lower than those of the Earth by 1 order of magnitude or more, with a typical dayside value of $0.6 \cdot 10^{16}$ el/m^2 [*Mendillo et al.*, 2013] or 0.6 TECu.

TEC can be determined by measuring the travel time difference for two signals with frequencies f_1 and f_2 along the same propagation path in the ionosphere (as is done on Earth for GPS [e.g., *Kintner and Ledvina*, 2005]). Due to electromagnetic dispersion within the ionospheric plasma, signals at different frequencies reach the receiver at different times. If this time difference is denoted as $\Delta\tau$, then TEC can be calculated using the following equation [*Kintner and Ledvina*, 2005], assuming that the difference between the two frequencies is small and the maximum plasma frequency of the ionosphere is much smaller than the two frequencies:

$$\mathrm{TEC} = \frac{c\Delta\tau}{40.3}\frac{f_1^2 f_2^2}{\left(f_2^2 - f_1^2\right)} \tag{2}$$

where c is the speed of light in vacuum.

TEC is useful in characterizing or monitoring the ionosphere. On Earth, for example, it affects satellite communications and position determination with Global Navigation Satellite Systems [e.g., *Pi et al.*, 1997; *Jakowski et al.*, 2001]. TEC measurements are used for ionospheric studies such as the analysis of solar activity effects or the monitoring of ionospheric equatorial anomalies [e.g., *Aarons et al.*, 1996; *Leitinger et al.*, 2000] or large-scale plasma redistribution through storms [e.g., *Mitchell et al.*, 2005]. Any system based on the propagation of radio waves through the ionosphere and performing accurate time delay measurements requires knowledge of TEC [*Klobuchar and Aarons*, 1973; *Budden*, 1985].

Since mid-2005, TEC has been estimated at Mars using data from the MARSIS (Mars Advanced Radar for Subsurface and Ionosphere Sounding) radar [*Picardi et al.*, 2004] on board Mars Express [*Chicarro et al.*, 2004]. This instrument is able to run in two operational modes. In the AIS (Active Ionospheric Sounding) mode [e.g., *Gurnett et al.*, 2005; *Morgan et al.*, 2013], MARSIS works as a topside ionospheric sounder. Ionograms from AIS are interpreted to obtain the electron density as a function of altitude between the main electron density peak and the spacecraft, i.e., the topside, which is then integrated to obtain TEC for the part of the ionosphere above the maximum density peak. In principle, TEC for the entire ionosphere can be estimated measuring the time delay of the surface echo, but the accuracy of this determination appears to be low [*Gurnett et al.*, 2008]. In the subsurface sounding mode, TEC is derived as a by-product from the analysis of signal distortion caused by the dispersive ionosphere [*Safaeinili et al.*, 2007; *Mouginot et al.*, 2008; *Cartacci et al.*, 2013].

MARSIS cannot operate in these two modes simultaneously. Therefore, comparison or intercalibration between the two data sets is usually done by comparing data acquired in different modes at closely spaced time intervals along an orbit. In some cases, MARSIS has operated using the two modes in an interleaved way, switching from one mode to the other every 5 min. The active ionospheric sounding mode provides TEC estimates only for the topside of the ionosphere, while in the subsurface sounding mode, TEC for the entire ionosphere can be obtained.

TEC estimates from subsurface data have been computed independently using two different methods: (1) the one explained in *Safaeinili et al.* [2003, 2007] and *Mouginot et al.* [2008], hereafter Mouginot et al., and (2) the method described in *Picardi et al.* [2008] and *Cartacci et al.* [2013], hereafter Cartacci et al. Both TEC methods are well-founded techniques largely used by the scientific community and based on wave propagation theory in the ionosphere (see previous references for more detail), which is characterized by the refractive index n, where

$$n(z) \cong \sqrt{1 - \frac{f_p^2(z)}{f^2}} \tag{3}$$

and z is the altitude from the surface of the planet, f is the MARSIS carrier frequency, and f_p is the plasma frequency. This last term can also be written as $f_p(z) = 8.98\sqrt{N_e(z)}$, where $N_e(z)$ is the electron density altitude profile. The ionosphere causes a frequency-dependent phase shift, $\Delta\varphi(f)$, that defocuses the subsurface radargram and is given by

$$\Delta\varphi(f) = \frac{4\pi f}{c}\int_{h1}^{h2} \Re(n-1)dh \tag{4}$$

where $\Re$ stands for the real part of the expression, c is the light speed in the vacuum, and h_1 and h_2 are the lowest and highest altitudes of the traversed path in the ionosphere. This equation takes into account the two-way propagation of the signal (spacecraft-planet-spacecraft). Equation (4) can easily be represented by a

Taylor expansion, from which TEC is obtained. However, the differences between both algorithms start here. On the one hand, the method of Mouginot et al. maximizes the signal-to-noise ratio (SNR) through the differential variation of the signal phase to obtain the best possible radargrams. This method uses a Chapman profile (equation (5)) to determine the initial values of the fitting for describing the ionospheric electron density profile, assuming that for one orbit, the neutral scale height, H, and the maximum electron density when the solar zenith angle is 0, n_o, are constants. Such that N_e is given by

$$N_e = n_o \exp\left[\frac{1}{2}\left(1 - \frac{h - h_o}{H} - Ch \cdot \exp\left(-\frac{h - h_o}{H}\right)\right)\right] \tag{5}$$

Here h_o is the height of the maximum production rate when the Sun is overhead (solar zenith angle 0), and Ch is the Chapman grazing incidence function [*Mouginot et al.*, 2008]. This method estimates H, n_o, and N_e, taking advantage of the Taylor expansion of equation (4), by doing an optimization of the SNR of the surface echo. Also, this method uses an external data set (surface range from the altimeter Mars Orbiter Laser Altimeter (MOLA) on board Mars Global Surveyor) to constrain the ionospheric correction. At the end of the process, the outputs are not dependent on any model. TEC estimates thus obtained are available at the Planetary Science Archive (PSA) of the European Space Agency (http://www.rssd.esa.int/index.php?project=PSA).

On the other hand, the algorithm of Cartacci et al. is based on the so-called contrast method [*Picardi and Sorge*, 2000], which was developed to correct phase distortion, and it is implemented in MARSIS onboard software, as well as in the ground processing software [*Picardi et al.*, 2004]. The TEC is not directly produced by the Contrast Method; it is obtained by the elaboration of the phase term a_2 (a quadratic phase term, equation (6)), where

$$a_2 = -\frac{4\pi}{c}\int_0^L \frac{f_p^2}{2\left(f_0^2 - f_p^2\right)^{\frac{3}{2}}} dz \tag{6}$$

is a direct output of the Contrast Method (equation (7))

$$a_2 \cong -\frac{4\pi}{c}\int_0^L \frac{1}{2}\frac{f_p^2}{f_0^3} dz = -\frac{2\pi}{cf_0^3}(8.98)^2 \int_0^L Ne \; dz \tag{7}$$

Here the integral limits h_1 and h_2 of equation (4) are considered as $h_1 = 0$ and $h_2 = L$, where L is the ionosphere thickness, f_0 is the central frequency of the radar signal band, and the last integral stands for the TEC. In this process, the shape of the signal main lobe (not the SNR) is optimized. At the end of the process, the outputs are not dependent on any model. The term a_2 is empirically estimated (see equations A1 and A2 in the Appendix of *Cartacci et al.* [2013]) from the initial value zero, used for the first step of the first frame processed by the Contrast Method. Since the Contrast Method was designed to work mainly during the nightside where the peak plasma frequency is much lower than the MARSIS carrier frequency, the approximation made from equations (6) and (7) yields a possible overestimation for the measurements with solar zenith angle smaller than 80°.

2. MARSIS TEC Discrepancy: Description of the Problem

The two TEC retrieval methods based on subsurface data should yield similar results, at least within the uncertainties of each method, since they use the same data set. However, significant differences in the results have been observed. Attempts to explain such differences using numerical simulations or TEC estimates based on other measurement techniques, such as radio occultation, have been so far unsuccessful.

Figure 1 shows different TEC estimates for Mars Express orbit 8712. Values from the subsurface mode obtained through the method of Mouginot et al. are shown as black dots, while values from the method of Cartacci et al. are plotted as red dots. TEC data from AIS topside profiles are marked by blue stars. In their turn, pink stars represent reconstructed TEC for the main ionospheric layer obtained by summing the contributions of the topside profile and a reconstructed Chapman bottomside [*Gurnett et al.*, 2008].

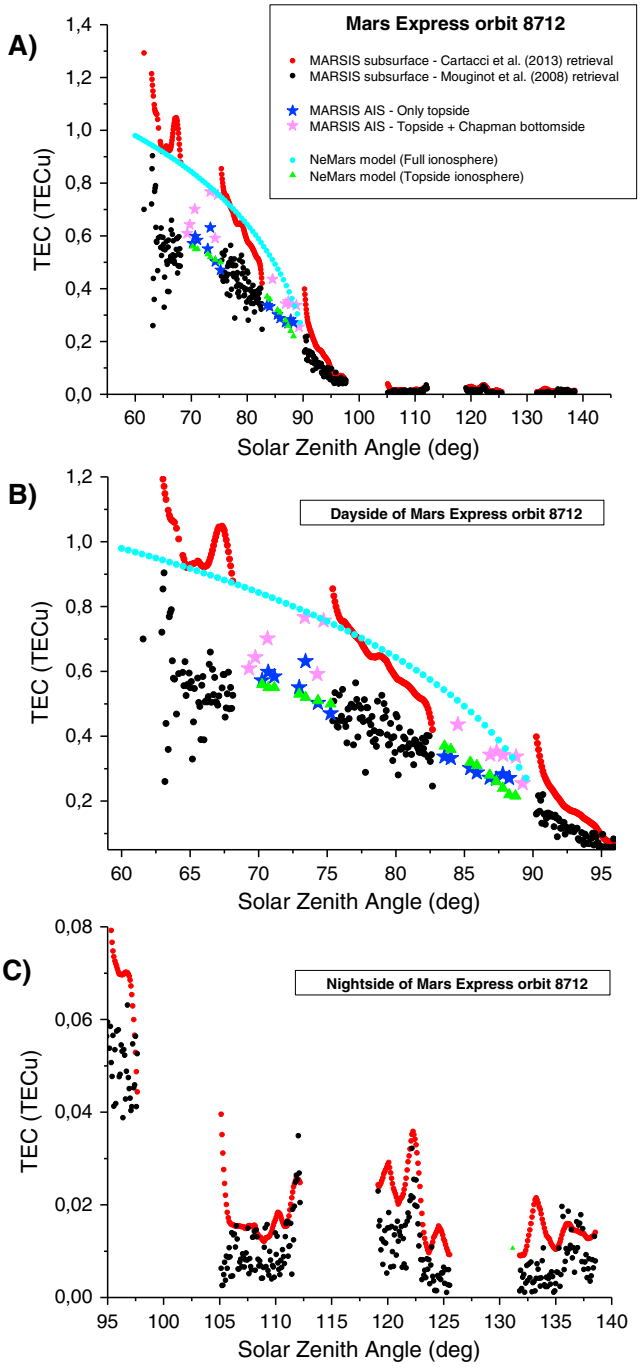

Figure 1. TEC intercomparison for Mars Express orbit 8712 (29 October 2010). (a) TEC data are plotted versus solar zenith angle: Mouginot et al.'s method (in black dots) and Cartacci et al.'s method (in red dots); from MARSIS AIS: straight topside profile integration (in blue stars) and from main layer (combination of the topside with a reconstructed Chapman bottomside (method explained at *Gurnett et al.* [2008]), in pink stars); and from the NeMars model [*Sánchez-Cano et al.*, 2013] for the entire ionosphere (in cyan dots) and only topside ionosphere (in green triangles). (b) Same figure focus on the dayside. (c) Same figure focus on the nightside.

Additionally, TEC from the numerical integration of an empirical model for the Mars dayside ionosphere has been included [*Sánchez-Cano et al.*, 2013]. This model is based on AIS data and radio occultation data from Mars Global Surveyor mission. The model was run for the entire ionosphere (in cyan dots) and for the topside ionosphere only (in green triangles).

It is important to note that TEC from the MARSIS subsurface mode is best taken on the nightside. On the dayside, this parameter is more difficult to retrieve because of dispersion delay, absorption, and attenuation as a result of the higher plasma frequency, and the separation of plasma frequency from operational frequency is therefore relatively small. It is for this reason that subsurface measurements are not taken when the solar zenith angle (χ or SZA) is lower than 60° [*Mouginot et al.*, 2008]. On the other hand, TEC from the MARSIS AIS mode is nonexistent or difficult to obtain on the nightside because the profile is not well detected at low plasma frequencies [see *Gurnett et al.*, 2008]. Thus, the only location where the best comparisons between both methods can be made is around the terminator.

It was expected that the two techniques for estimating TEC based on the subsurface data would broadly agree and that the AIS-derived TEC would be about 30% lower for a solar zenith angle of 60° (estimated values from radio occultation profiles; see also Discussion section and Figure 10). However, the two methods based on subsurface data produce similar results only at night and close to the terminator, while they differ significantly in the dayside, with increasing discrepancy at decreasing solar zenith angles. Furthermore, TEC computed from MARSIS AIS data is not consistent with that obtained through Mouginot et al.'s method, because they have practically the same value while AIS measures only the topside ionosphere. TEC values from Cartacci et al. seem to match better the MARSIS AIS data and

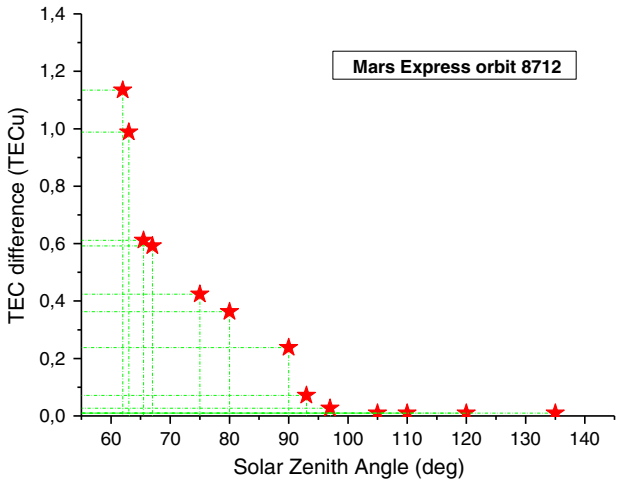

Figure 2. Absolute differences between the maximum and minimum TEC values of all estimates that appear in Figure 1 (Mars Express orbit 8712) for every solar zenith angle. The scatter clearly increases on the dayside. All methods converge in the nightside beyond the terminator ($\chi > 90°$). On the dayside, the discrepancy can be up to 1 TECu at solar zenith angle of 60°, which is the same order of magnitude as the TEC value itself.

the NeMars model, although Cartacci et al. acknowledge that their method overestimates TEC on the dayside. On the other hand, the green triangles and blue stars are right on top of one another, implying substantial agreement between the model and MARSIS AIS results. All in all, different data and techniques provide different results for the TEC, leading to substantial confusion of what the real value should be.

The absolute difference between the maximum and minimum TEC values for all estimates of Figure 1 (Mars Express orbit 8712) and for each solar zenith angle are plotted in Figure 2. The scatter clearly increases on the dayside. All methods converge in the nightside beyond the terminator. On the dayside, the discrepancy can be up to 1 TECu at solar zenith angle of 60°, which is the same order of magnitude as the TEC value itself. It is important to remark here that the level of uncertainty is difficult to estimate, since the TEC is a by-product of a very complex data processing technique (see Discussion section).

From these observations, the following preliminary conclusions can be drawn:

1. The maximum difference of TEC among all the data set and techniques can be easily up to 1 TECu on the dayside.
2. On the nightside, the data are more consistent, although the differences can remain a factor of 2.
3. The discrepancy in the results processed from the same data set with two different techniques is of concern. Mouginot et al.'s method does not suffer from the same approximation as Cartacci et al.'s method and is expected to be more robust. However, this method produces results that are inconsistent with topside sounder data. On the contrary, although the method by Cartacci et al. is expected to overestimate the dayside TEC by about 10% because of some approximations of the contrast method (see *Cartacci et al.* [2013] and Discussion section), it produces results that are consistent with topside sounder estimates.

Moreover, *Lillis et al.* [2010] showed that the behavior of Mouginot et al.'s data could be reproduced fairly well using the general Chapman theory. *Mendillo et al.* [2013] compared a 2 year sample of this data set with the TEC computed using a one-dimensional ionosphere model [*Mendillo et al.*, 2011], with the aim of studying the ionospheric variability. This model was run for two specific intervals of local time and for two of latitude, getting an acceptable agreement in morphology patterns for such average conditions. Their main conclusion was that model-data comparisons were reasonably successful. Similarly, *Campbell et al.* [2014] in a first approximation compared this data set with the TEC obtained from the subsurface radar SHAllow RADar (SHARAD) [*Seu et al.*, 2007] on board Mars Reconnaissance Orbiter probe, concluding that the maximum average TEC value from SHARAD observations for solar zenith angles near 30 and 90° agrees well with Mouginot et al.'s TEC measurements from Mars Express.

3. Statistical Analysis

In order to advance further the understanding of the variability in the MARSIS data sets, a statistical analysis has been carried out. Nineteen Mars Express orbits with MARSIS data acquired in both operational modes were selected, five of them belonging to a special interleaved mode campaign, which the Mars Express project runs specifically for this purpose. The list of orbits is available in Table 1.

Table 1. Information Related to the 19 Mars Express Selected Orbits[a]

Mars Express Orbit Number	Date	$F_{10.7}$ (Solar Flux Unit, sfu)	d_{M-S} (AU)	Ls (deg)	Belonging to Interleave Mode Campaign
4210	16-04-2007	69	1.40	220.2	No
4214	17-04-2007	69	1.40	220.9	No
4215	17-04-2007	69	1.40	221.1	No
4219	19-04-2007	68	1.40	221.8	No
4221	19-04-2007	68	1.40	222.1	No
5295	15-02-2008	70	1.63	32.3	No
5299	16-02-2008	70	1.63	32.8	No
6458	12-01-2009	69	1.44	190.0	No
6461	13-01-2009	71	1.44	190.5	No
6462	13-01-2009	71	1.44	190.7	No
6581	16-02-2009	70	1.41	211.1	No
6587	18-02-2009	70	1.41	212.1	No
6592	19-02-2009	69	1.41	213.0	No
6598	21-02-2009	71	1.41	214.1	No
8712	25-10-2010	86	1.49	169.7	Yes
8761	8-11-2010	84	1.47	177.6	Yes
9466	01-06-2011	114	1.43	303.4	Yes
9528	19-06-2011	99	1.45	314.0	Yes
9531	20-06-2011	96	1.45	314.5	Yes

[a]Orbit number is marked in the first column, terrestrial date of the measurement in the second column, $F_{10.7}$ index as proxy of the solar activity in the third column ($1\ \text{sfu} = 10^{-22}\ \text{Wm}^{-2}\ \text{Hz}^{-1}$), Mars heliocentric distance in the fourth column, solar longitude in the fifth column, and an indication of the orbit belonged to the special Mars Express interleave campaign carried on to compare TEC from both operational modes in the sixth column.

3.1. MARSIS Subsurface Mode Data Sets

The signal distortion due to the ionosphere is a problem for the MARSIS subsurface mode. Thus, MARSIS measurements for solar zenith angle lower than 60° are usually avoided [*Mouginot et al.*, 2008]. To see the effect of the solar illumination on the data, TEC from Cartacci et al. and Mouginot et al. for the 19 selected orbits have been compared (Figures 3 and 4). Since subsurface data are based on the signal-to-noise ratio (SNR), which is computed by taking the ratio between the brightest echo within a frame with the average power of the background noise, a data quality indicator or "flag" is provided on the data files. A value of 1 means that the SNR is greater than 15 dB (considered good data), while a value of 0 means that the SNR is lower (considered bad data). Data with flag 0, effectively an SNR less than 15 dB, have not been considered in this study. In addition to flagged data that are suspect, the data set of Cartacci et al. occasionally includes unexplained large and narrow spikes in TEC. To our knowledge, these spikes are not related to any ionospheric phenomena, and for that reason, in this comparison, the spikes have also been omitted from further analysis.

The final data used in this work were split into three different solar zenith angle intervals: dayside ($60° < \chi < 75°$), dayside/terminator ($75° < \chi < 90°$), and nightside ($\chi > 90°$). The amount of useful data from these orbits is 6232 TEC values for the dayside, 2003 for the dayside/terminator, and 2538 for the nightside. In Figure 3, the absolute differences of the TEC from Cartacci et al. and Mouginot et al.'s methods for the 19 selected orbits are presented. Figure 3c shows that for $\chi > 90°$, there are no significant differences between the two methods: the mean and median of the absolute differences are less than 0.007 TECu with a standard deviation of 0.05 TECu. It indicates that both methods agree extremely well for the nightside data, when the distortion effect of the ionosphere is not substantial. Close to the terminator, $75° < \chi < 90°$, where the day-to-night ion transport can be significant (Figure 3b), a slight difference starts to appear between the two methods: an average difference of 0.09 TECu for the mean and median absolute variations and the standard deviation of the differences is 1 order of magnitude higher, reaching 0.11 TECu. However, these differences are small enough to be considered within the margin of error (see Discussion section), and the increment by 1 order of magnitude most likely is due to the ionosphere developing during dawn/dusk conditions. The dayside is where the discrepancy is most noticeable (Figure 3a). Here the mean and median of the absolute differences reach

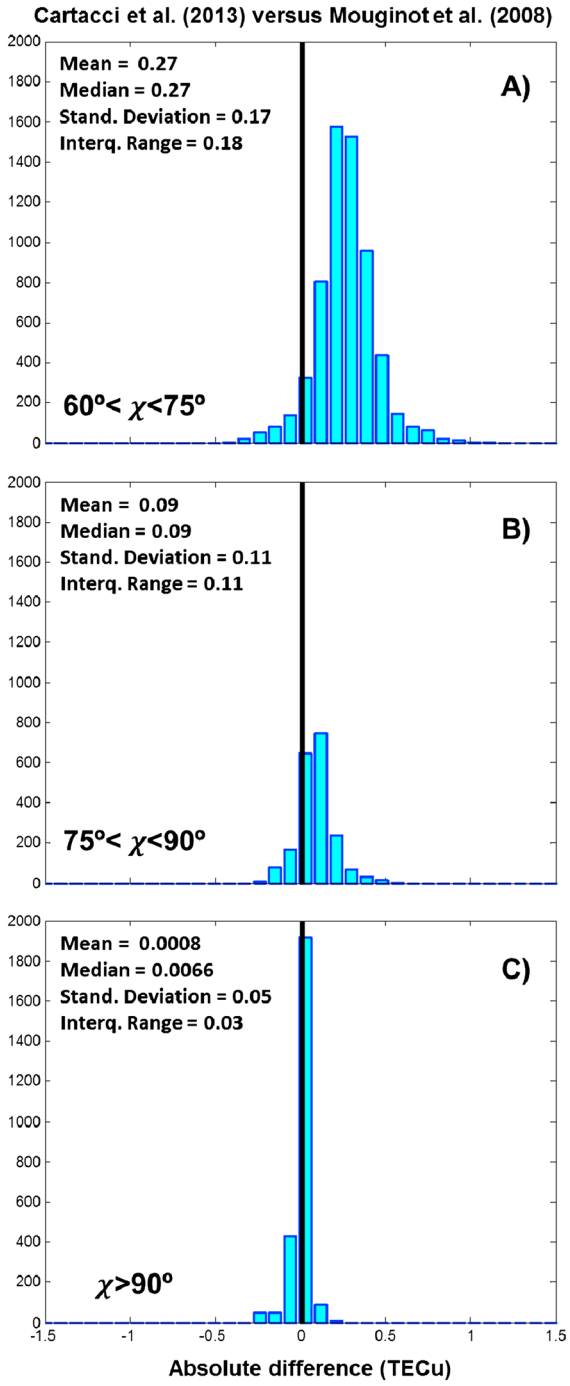

Figure 3. Absolute differences of the 19 selected orbits between Cartacci et al. and Mouginot et al.'s data for three different solar zenith angle intervals: (a) dayside ($60° < \chi < 75°$) (top, amount of data 6232), (b) dayside/terminator ($75° < \chi < 90°$) (medium, amount of data 2003), and (c) nightside ($\chi > 90°$) (bottom, amount of data 2538). The vertical black line marks the zero difference, and the units are in TECu. During nightside and close to the terminator when the disturbing effect of ionosphere is not substantial, both methods agree well. The discrepancy rises on the dayside, where the ionospheric distortion in the electromagnetic signals is evident.

0.27 TECu, with a dispersion characterized by a standard deviation of 0.17 TECu. Clearly, the differences can be attributed to the dayside ionosphere, the effects of which are not well interpreted by the retrieval algorithms. This discrepancy is large and can be higher than a third of 1 TECu, which is 30% of the typical TEC value on the dayside. Furthermore, the ionospheric distortion in the electromagnetic signals can be observed in the data spread: the standard deviation is 1 order of magnitude higher in the case of the dayside compared with that for the nightside. This is probably due to the effects of the dayside ionosphere, because the frequencies used by MARSIS on the dayside are closer to the maximum plasma frequency than on the nightside and because TEC shows a large day-to-day variability on the dayside [see, e.g., *Withers et al.*, 2012].

Finally, these two data sets have been compared by plotting their ratio (Figure 4, top), which can be useful to look for systematic trends. The ratio departs from the 1:1 dependence (black dashed line) and is equal to about 1.41, with a larger scatter on the dayside. In fact, when only data from night and terminator (green and red points) are considered, the ratio is 1.14, considerably closer to the expected 1:1 dependence. The ratio values are the slope of the best fit lines. If in the future, the comparison between the two techniques is carried out, from a theoretical or simulation point of view, it would be useful to see whether a similar ratio can be found. However, in this plot, a group of points are observed clearly far away from the general trend. These data, which have been plotted separately in Figure 4 (bottom), correspond to the Mars Express orbit 6458. While in the daytime, the results for this orbit are consistent with the ratio obtained in Figure 4 (top) in the terminator, and in the nighttime, Mouginot et al.'s technique provides TEC values higher than Cartacci et al.'s This fact is peculiar since for solar zenith angles higher than 75°, both algorithms are expected to be more robust because of the weak plasma ionization.

3.2. Subsurface Mode MARSIS Data Versus AIS Mode MARSIS Data

Here we investigate the TEC from the two algorithms using the subsurface mode with TEC estimates from the AIS mode. For a given Mars Express orbit, the heliocentric distance, solar

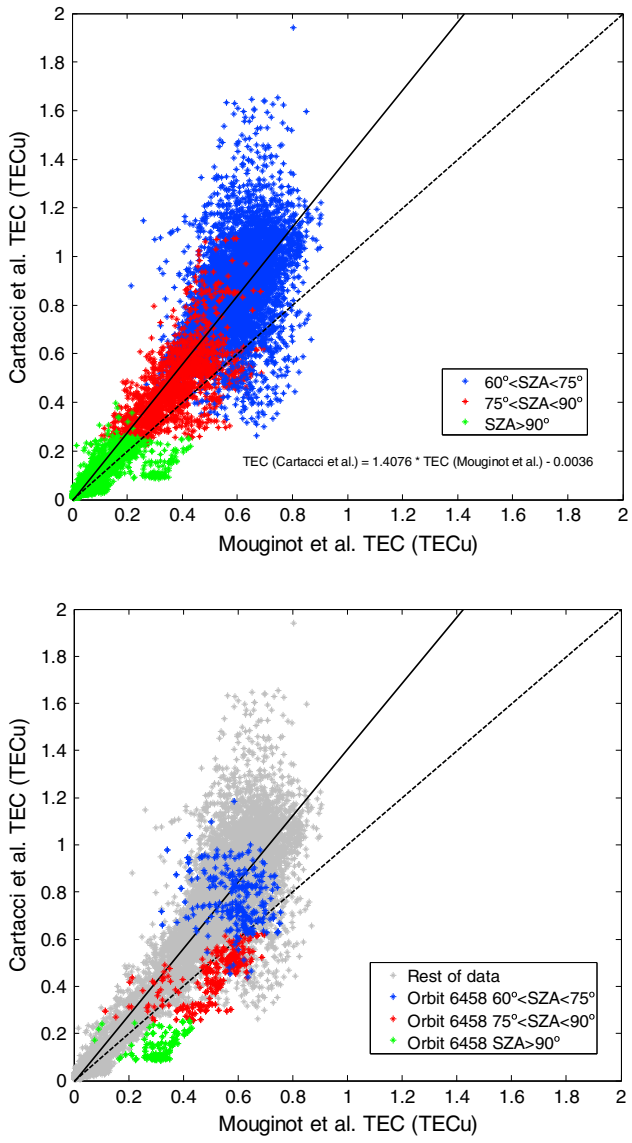

Figure 4. (top) TEC (Cartacci et al.) versus TEC (Mouginot et al.). Data have been split into three different solar zenith angle intervals: dayside in blue ($60° < \chi < 75°$), dayside/terminator in red ($75° < \chi < 90°$), and nightside in green ($\chi > 90°$). The dashed black line shows the 1:1 dependence, while the solid black line represents a ratio of 1.4076 between the two data sets. (bottom) Same figure than before but only with the orbit 6458 shown in colors, while the rest of data (data from 18 orbits) is plotted in grey in the background. TEC is always represented in TECu.

longitude, and solar activity values are the same; the latitude and solar zenith angle are the only parameters that vary. For the 19 selected orbits (Table 1), ionospheric and subsurface measurements are consecutive. This means that they were never acquired at the same time. This characteristic, although useful to visually examine the consecutive data, can be a weakness in the statistical comparison. Therefore, to compare data acquired in subsurface and ionospheric modes at the same position, it has been decided to compute the best fit to the subsurface data. Then, an interpolation/extrapolation of this best fit curve was done for the solar zenith angle or latitude condition of all ionospheric data (Figure 5).

In order to minimize the error introduced in the comparisons doing the data best fit, every case has been analyzed carefully. Since the only two parameters that vary along one orbit are the solar zenith angle and latitude, the same study has been done for both varying parameters, i.e., TEC versus solar zenith angle and versus latitude (Figures 5a and 5b, respectively). This approach ensures that the results are consistent regardless of the representation. All data have been fitted with a second-degree polynomial. However, in some particular cases (e.g., orbit 9531 (Figure 5)), when the nightside and dayside fits were very different, the fit has been done only for solar zenith angles smaller than 100°.

Figure 6 shows the results of these comparisons. The same procedure has been performed with subsurface data from Mouginot et al. and Cartacci et al.'s retrieval methods. In total, there were 458 AIS data points belonging to the 19 selected orbits (Table 1). The analysis confirms that the mean and median of the absolute differences between ionospheric data from AIS mode and Mouginot et al.'s subsurface data are very small, both for latitude and solar zenith angle configurations. The mean difference is less than 0.02 TECu, and the median difference is practically zero. The standard deviation of these differences is 0.12 TECu, consistent with the histogram shape and with the interquartile range. This means that the method of Mouginot et al. gives practically the same value as the topside ionogram MARSIS TEC. On the other hand, the absolute differences between topside ionospheric data from the AIS mode and Cartacci et al.'s subsurface data are higher by 2 orders of magnitude: an absolute difference of ~0.35 TECu, equivalent to a relative difference of ~35%, where Cartacci et al.'s values are higher.

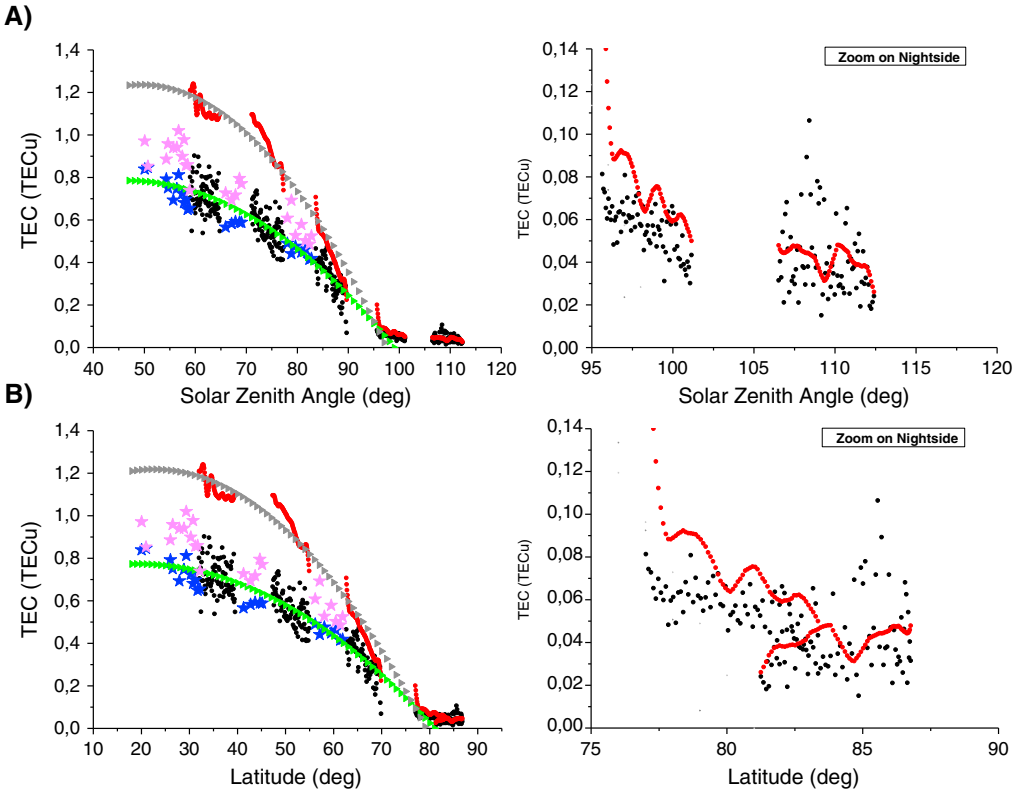

Figure 5. (a) TEC solar zenith angle variation and (b) TEC latitude for Mars Express orbit 9531 (26 June 2011), which belongs to the Mars Express "MARSIS interleaved mode" campaign. (Figures 5a and 5b, left) The TEC derived from MARSIS subsurface mode—black dots from Mouginot et al.'s method and red dots from Cartacci et al.'s method—has been represented with the topside AIS-derived TEC (blue stars) and with the TEC from the main layer (AIS data plus Chapman best fitting for the bottomside, pink stars). Moreover, the best fitting curves for Mouginot et al.'s method (green triangles) and for Cartacci et al.'s method (grey triangles) have been plotted. (Figures 5a and 5b, right) Zoom on the nightside data.

3.3. Model Comparison

A possible explanation for the discrepancy between the two subsurface data sets is the presence of secondary peaks below the main peaks. Since there are no coordinated observations that allow the estimation of these peaks, the use of a model is necessary. The subsurface data sets are compared with the NeMars empirical model [*Sánchez-Cano et al.*, 2013]. NeMars models the dayside Martian ionosphere assuming that it is made of two layers. The upper layer is modeled based on the data from the Active Ionospheric Sounding mode of MARSIS instrument (and therefore is in excellent agreement with the AIS data by design) and the secondary one based on radio science data from the Mars Global Surveyor mission. In Figure 7, three examples of NeMars electron density profiles have been plotted with their corresponding MARSIS AIS electron density profile. The final output is the electron density profile, which can be easily numerically integrated to obtain TEC. Since the main layer model is based on AIS data, the model was not compared with this data set because by design, a good agreement is expected. The model has been only compared with Mouginot et al. and Cartacci et al. TEC estimates to analyze if the contribution of the bottomside is the reason for the main difference between both subsurface algorithms.

TEC has been calculated with the NeMars model using the same values for solar zenith angle, solar activity, and heliocentric distance (inputs of the model) for the selected orbits. An example is shown in Figure 8, where the TEC values are displayed together with the modeled TEC. The discrepancies have been quantified with another statistical study of the differences between both modeled TEC data and subsurface data (Figure 9). To see the effect of the solar illumination, data have been again split into three solar zenith angle intervals as in the previous section. The comparison has been carried out between the modeled TEC and the subsurface TEC data, Mouginot et al.'s panels A and C and Cartacci et al.'s panels B and D, in two of the three solar zenith angle intervals: dayside ($60° < \chi < 75°$, panels A and B) and dayside/terminator

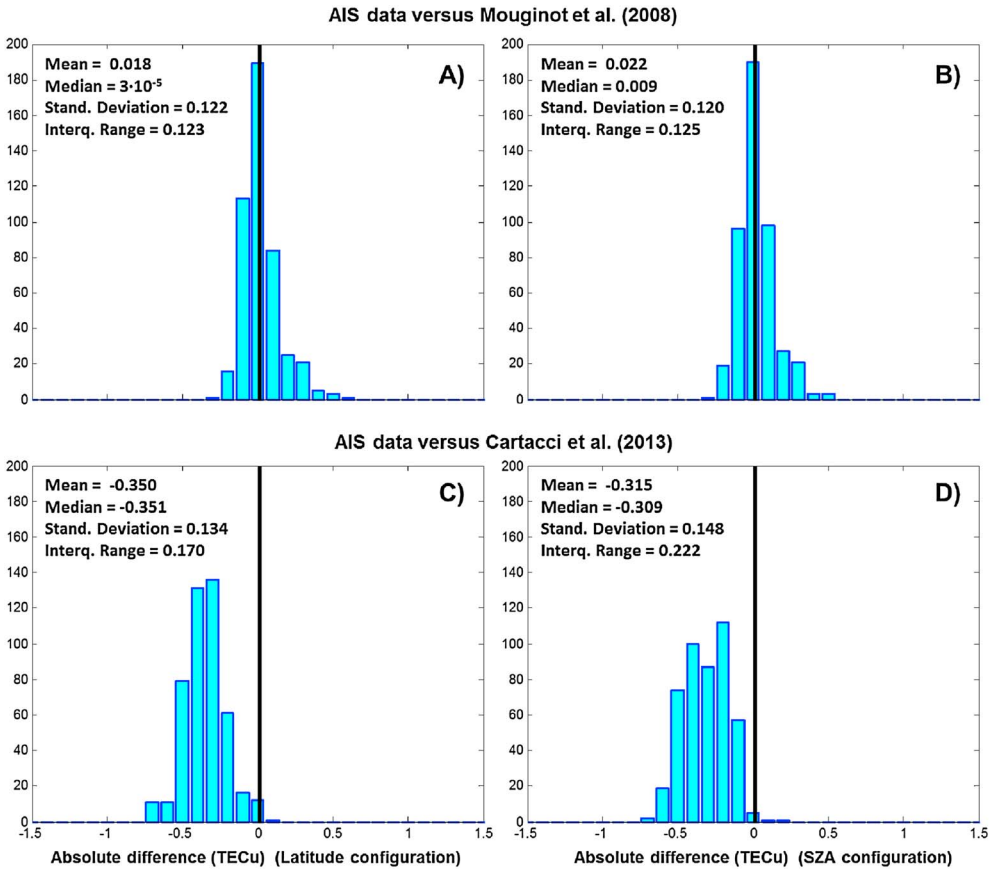

Figure 6. Absolute differences between the topside AIS-derived TEC and the TEC retrieved from the MARSIS subsurface mode: (a and b) Mouginot et al.'s method and (c and d) Cartacci et al.'s method. The total number of data points is 458 (19 orbits). (Figures 6a and 6c) Histograms of the absolute differences in TECu for the latitude as the varying parameter. (Figures 6b and 6d) Histograms of the absolute differences in TECu for the solar zenith angle as the varying parameter. The vertical black line marks the zero difference. The analysis confirms that the absolute differences between ionospheric data from AIS mode (topside ionosphere) and Mouginot et al.'s subsurface data (full ionosphere) are practically nonexisting, being a clear inconsistency (Figures 6a and 6b). The absolute differences between ionospheric data from AIS mode and Cartacci et al.'s subsurface data are higher (Figures 6c and 6d). It seems more realistic, although it is known that this latest subsurface retrieval overestimates the dayside TEC.

($75° < \chi < 90°$, panels C and D). Comparisons for the nightside were not possible here since the model works for $\chi < 90°$ only. Figure 9 displays the histograms and the results of the comparisons. For the solar zenith angle range of $75° < \chi < 90°$, absolute values of the model NeMars and Cartacci et al.'s method appear to match well: the mean and median of the absolute difference reach 0.09 TECu, with a small standard deviation of 0.09 TECu. However, there is a small systematic difference with respect to the model. Comparing the NeMars TEC estimates with those from Mouginot et al.'s, the mean and median of the absolute difference are less than 0.19 TECu. These results corroborate the one obtained in the previous section (Figure 5), which is that, close to the terminator, all data sets give a close and consistent value of the total electron content. For the range of $60° < \chi < 75°$, the ionosphere obviously has a significant effect on the signal dispersion, and as a result, the algorithms have pronounced difficulties to obtain the real TEC. This is supported statistically in Figure 9, where Mouginot et al.'s values are on average 0.35 TECu lower than the model values. On the contrary, Cartacci et al.'s values are very close to the expected modeled TEC, with a mean and median difference of 0.09 TECu and with a small spread of the data set (standard deviation of 0.16 TECu).

4. Discussion

The total electron content (TEC) is a useful physical quantity for describing and monitoring the Martian ionospheric variability because it contains information on the total amount of free electrons. This parameter

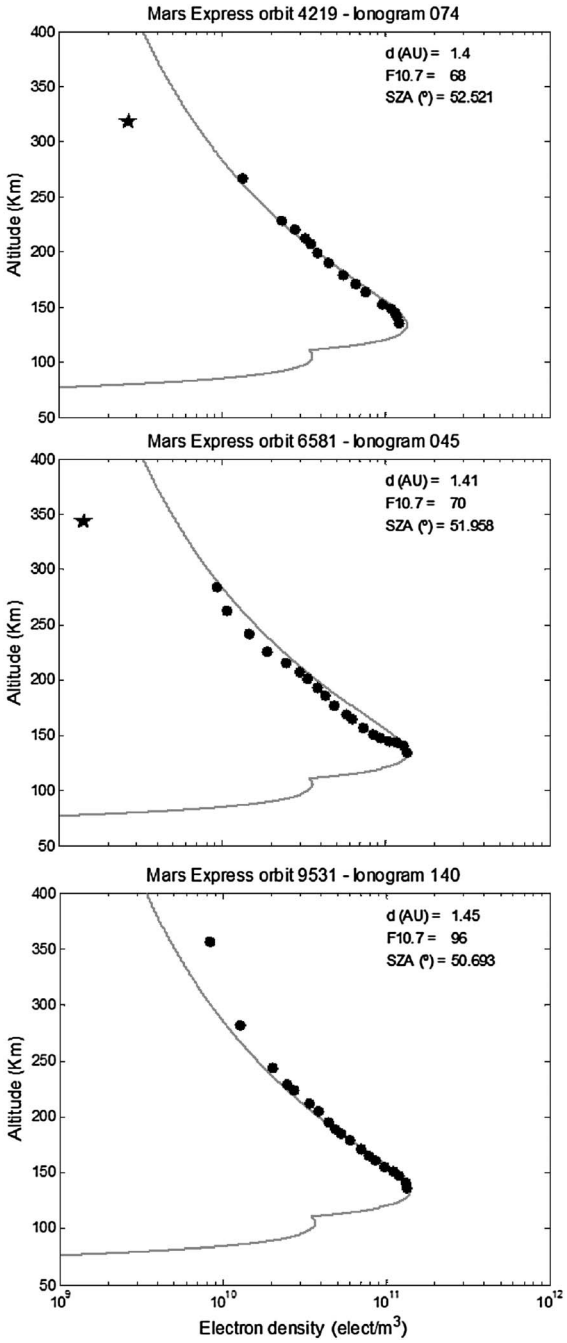

Figure 7. (top, middle, and bottom) Three examples of NeMars electron density profiles (in grey) run for the conditions of each MARSIS AIS electron density profile (black dots). The black stars stand for the local plasma at the spacecraft altitude. The star is not visible in the bottom because of the window size: it is localized at 510.3 km of altitude and $1.8 \cdot 10^8$ el/m^3 of local density.

is routinely derived from the Mars Express MARSIS radar. TEC estimates from the subsurface sounding mode can be computed from the same raw data independently using different algorithms, which should yield similar results. However, significant differences especially on the dayside have been found between the TEC values estimated by Mouginot et al.'s and Cartacci et al.'s methods. Moreover, both algorithms seem also to disagree with the TEC results from the AIS mode. The present statistical study has quantified the mismatch between the various ways in which the TEC can be derived from the MARSIS observations. In order to help to understand which of the algorithms for subsurface mode gives the best estimate of TEC, a comparison between the results given by the empirical model of the Martian ionosphere developed by *Sánchez-Cano et al.* [2013] and the different data sets has been performed.

All signs seem to indicate that the maximum plasma frequency of the ionosphere is the key factor of this data set discrepancy. At nightside and in the dawn and dusk regions where there is low plasma ionization, the two algorithms are consistent. However, in the full dayside, the operational MARSIS frequencies (1.8, 3, 4, and 5 MHz, with a bandwidth of 1 MHz for each frequency) are very close to the maximum plasma frequency, which causes strong interferences in the returned signal from the surface of the planet and therefore could be a possible explanation for the nonagreement on the TEC value. Furthermore, while the physics that underpins both algorithms is the same, wave propagation in the ionosphere, the assumptions of each algorithm are different and could be the key to such TEC discrepancy.

An important consideration is the possible overestimation of Cartacci et al.'s TEC. Their TEC is systematically the largest. They affirm that the Contrast Method somehow overestimates the results in the dayside [*Cartacci et al.*, 2013], appearing less reliable in this region of the ionosphere by a factor still to be quantified. In principle, Cartacci et al. suggest that their method yields an overestimation of the absolute value of a_2 (which is a parameter directly related to TEC) on the order of $1.5(f_p/f_0)^2$, which for a plasma frequency of $f_p = 1$ MHz and a carrier frequency of $f_0 = 4$ MHz, is about 10%. The work shown in this paper, however, indicates that at $\chi = 60°$, the difference between Cartacci et al. and Mouginot et al. is about 30%. Despite this possible overestimation, Cartacci et al.'s method seems to be consistent with the NeMars model and with AIS data. In addition, it seems that Mouginot et al.'s algorithm can overestimate the TEC

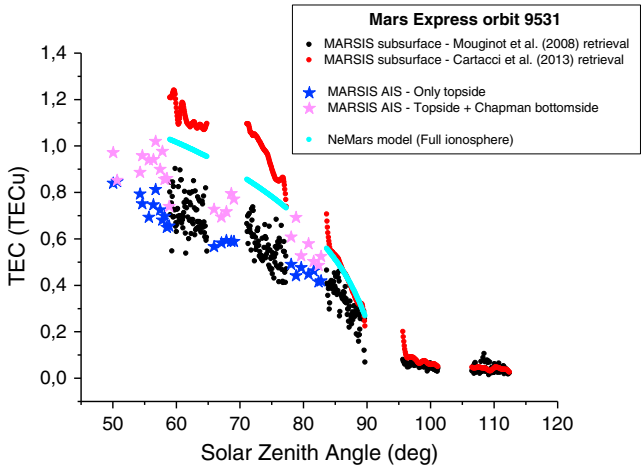

Figure 8. TEC solar zenith angle variation for Mars Express orbit 9531 (26 June 2011, same as in Figure 5), which belongs to the Mars Express MARSIS-interleaved mode campaign. The TEC derived from the MARSIS subsurface mode (black dots from Mouginot et al.'s method and red dots from Cartacci et al.'s method) have been represented with the topside AIS-derived TEC (blue stars). The modeled NeMars TEC for the full dayside ionosphere is plotted with cyan dots. A zoom of the nightside data has been incorporated.

value for some specific conditions, for example, the data from the orbit observed in Figure 4 (Mars Express orbit 6458). The Mouginot et al.'s TEC of this particular orbit is clearly different from the typical values for solar zenith angles higher than 75°, where both subsurface algorithms are more robust.

On the other hand, when TEC from the subsurface operational mode (entire ionosphere) is compared with TEC from AIS mode (only topside ionosphere), one expects that TEC from subsurface measurements will be higher. TEC estimates from AIS topside measurements ignore the bottom of the main layer and all of the secondary layer, which account for approximately 24–29% of the TEC (Figure 10a). We would therefore expect the AIS topside TEC to be less than the actual TEC. However, it appears to agree with the result of Mouginot et al. as can be seen in Figure 6. Is Mouginot et al.'s estimate too low or is the AIS topside too high? Does this good agreement mean that most of the TEC value is due to the ionosphere above the main peak? It is well known that the two main layers of the Martian ionosphere are similar to the *E* region of Earth's ionosphere, where the production of ions is equal to the ion losses due to photochemical equilibrium [*Mouginot et al.*, 2008]. This fact would imply a fast decay of the electron density below the peak (see Figure 5.5.1 of *Rees* [1989]). However, on one hand, Cartacci et al. do not confirm this statement (Figure 6). Similarly, although the ionospheric variability is high, Mars Express radio occultation profiles show a clear contribution to the bottomside under the main peak [e.g., *Withers et al.*, 2012]. On the other hand, as mentioned before, the estimated TEC contribution of the ionospheric bottomside by the NeMars empirical model is between 24 and 29% (Figure 10a), which is not negligible. This percentage is the addition of the secondary layer, which contributes between 0 and 11% in TEC (Figure 10c) and the contribution of the bottomside of the main layer, which is between 18 and 24% (Figure 10b). This latest quantity is empirically represented in Figures 1, 5, and 7, where the pink stars denote TEC of the main ionospheric layer (AIS data with Chapman layer fit for estimation of the bottomside) and the blue stars denote TEC only of the topside (just AIS data). The difference between these two sets of data is the TEC contribution of the main layer bottomside. The AIS TEC is only slightly higher than Mouginot et al.'s version when the bottomside is added in (pink stars). Is the model overestimating the bottomside? At this point, it is important to remember that NeMars is a semiempirical model created by fitting data and considering Chapman functions as the best representation of the ionosphere. The only inputs are the solar zenith angle, the solar activity, and the heliocentric distance. However, other factors like the ionospheric chemistry, neutral atmosphere, or other ionization sources like particle precipitation are not considered as inputs. This could yield in a variability below the main peak which could be not addressed by the NeMars model. If we assume that the topside sounder provides correct values and that the contribution to the TEC of the bottomside is not negligible (on the order of 24–29%, Figure 10), does that mean that Mouginot et al.'s method underestimates the TEC? If so, why?

The answer to this question is more challenging if one takes into account that in a first approximation *Campbell et al.* [2014], compared the subsurface Mouginot et al.'s data set with the TEC obtained from the subsurface radar SHARAD [*Seu et al.*, 2007] on board Mars Reconnaissance Orbiter probe and state that the maximum average TEC value in SHARAD observations is about $0.8 \cdot 10^{16}\,\mathrm{m}^{-2}$ for solar zenith angles near 30° and the average value near $\chi = 90°$ is about $0.19 \cdot 10^{16}\,\mathrm{m}^{-2}$. Both values agree well with estimates of the Mars Express TEC at similar solar zenith angles from Mouginot et al.'s method. If these values are superimposed in Figure 4 of this paper, both measurements can be localized inside the data cloud, although

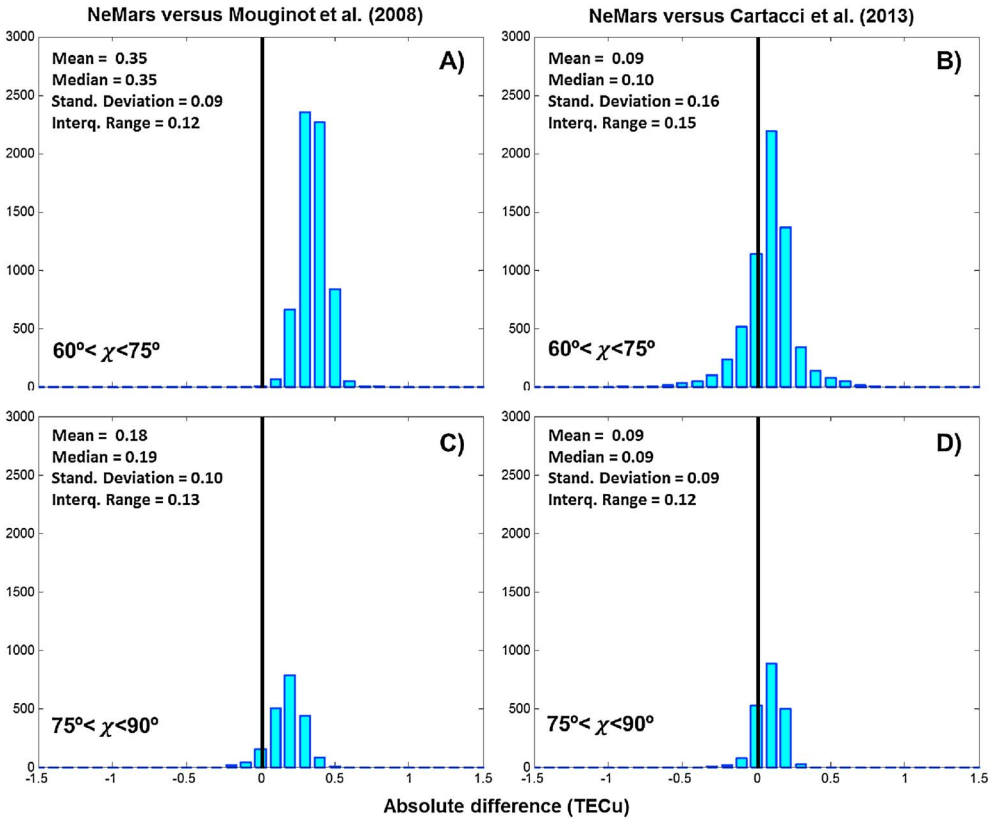

Figure 9. Absolute differences between TEC from the entire dayside NeMars model and TEC from subsurface mode: (a and c) Mouginot et al and (b and d) Cartacci et al.. Data were split into two solar zenith angle intervals: (Figures 9a and 9b) dayside ($60° < \chi < 75°$) and (Figures 9c and 9d) dayside/terminator ($75° < \chi < 90°$). Nightside is not compared since NeMars model only works for the dayside ionosphere. The vertical black line marks the zero difference. The difference between the model and (Figures 9b and 9d) Cartacci et al. is constant for both solar zenith angle situations being small (mean 0.09 TECu). On the contrary, the difference between the model and (Figures 9a and 9c) Mouginot et al. is substantial in the dayside, reaching differences of 0.35 TECu for the mean.

the value for the solar zenith angle of 30° is not very trustworthy since the MARSIS subsurface mode does not work in the full dayside. Similarly, Mouginot et al.'s data were successfully compared with other models such as the photochemical model of *Mendillo et al.* [2011, 2013]. This model calculates the density, velocity, and temperature of the chemical ionospheric species as a function of the altitude, latitude, and time. The model-data comparisons showed that in general, there is a reasonably successfully agreement in morphology patterns. However, from Figure 9 of *Mendillo et al.* [2013], some specific differences can be inferred. For subsurface measurements at latitudes between 10 and 20°N, the agreement is excellent for local times between 8 and 24 h but not for local times on the nightside between 0 and 8 h, where the model underestimates the TEC by a factor up to 0.4 TECu. This may be due to the model not accounting for electron precipitation on the nightside. On the contrary, for latitudes between 70 and 80°N, the model outputs overestimate the subsurface Mouginot et al.'s TEC for all local times; the difference on the nightside can be up to 0.3 TECu higher. As discussed by *Fox* [2009], the reason could be the horizontal winds at these latitudes. Moreover, in the same figure, the model TEC is compared with latitude for two specific intervals of local time. Again, the agreement in general is quite good, with an exception in the south hemisphere between 30 and 70°, where the model overestimates TEC by a factor up to 0.3 TECu. Therefore, does it mean that in some of these cases, where the model overestimates Mouginot et al.'s TEC, the model is in agreement with Cartacci et al.?

Additionally, the model of *Mendillo et al.* [2011] and Mouginot et al.'s TEC have also been successfully compared with radio occultation data. Particularly, Figure 8 of *Mouginot et al.* [2008] shows a comparison of their TEC with radio science measurements obtained by other missions like Mariners, Mars, Vikings, Mars

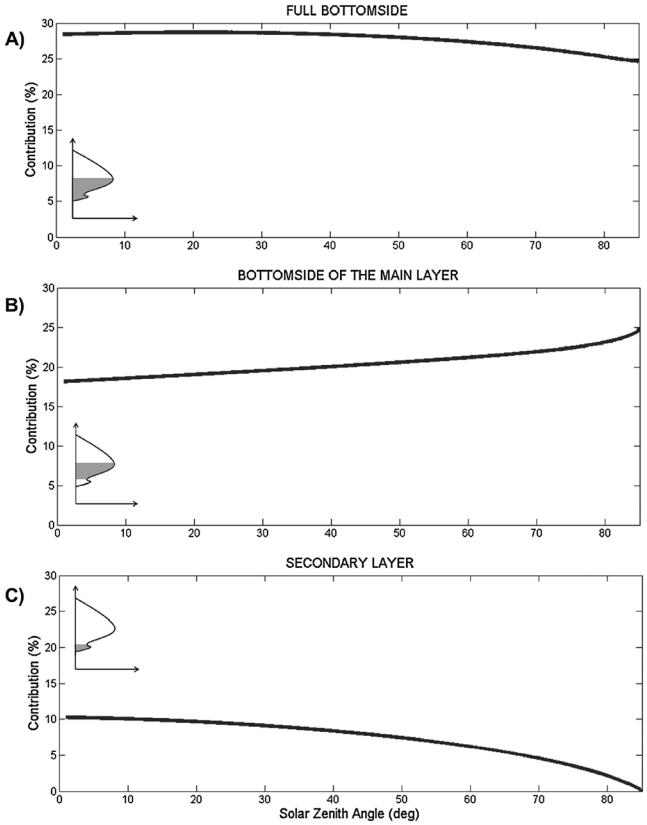

Figure 10. TEC contribution in percentage calculated from the empirical model NeMars for dayside solar zenith angles. (a) Contribution of the full bottomside (from main peak altitude to the ground). (b) Contribution of the bottomside of the main layer (from main peak to the cross-point altitude with the secondary layer). (c) Contribution of the secondary layer (from cross-point altitude with the main layer to ground). In all cases, a schematic electron density profile has been included where the area contribution of the profile is highlighted in grey.

Global Surveyor, or Mars Express. The agreement is very good since most of the data were taken for high solar zenith angles, with the exception of TEC from Mariner 9, where there is a difference at solar zenith angles of 50° of around 0.3 TECu, although this could be due to differences in solar activity conditions. However, it is important to consider that the topside shape of the electron density profile from radio occultation and from the MARSIS radar is different (see Figure 3 of *Morgan et al.* [2008] and Figures 3 and 4 of *Sánchez-Cano et al.* [2012]), being correctly reproduced with a constant neutral scale height (like the normal Chapman profile) in the case of radio occultation and with an altitude-variable neutral-scale height in the case of MARSIS radar [*Sánchez-Cano et al.*, 2013]. Although this main discrepancy can in principle be attributed to the differences in accuracy between the two techniques [*Gurnett et al.*, 2008], it could also be a consequence of different geometrical assumptions for the atmospheric stratification. Furthermore, the MARSIS radar provides measurements specific to a particular vertical raypath, while radio occultation requires integration along a horizontal path that may sample widely differing conditions and requires many corrections, such as the Earth's ionosphere-troposphere contribution or the trajectory of the signal in the solar wind. A typical radio occultation profile can be fairly well represented with a Chapman layer (constant neutral scale height), which clearly differs from MARSIS AIS profiles (see Figure 13 of *Němec et al.* [2011], where the derived neutral-scale height is seen to vary with the solar zenith angle). Therefore, topside TEC from both kinds of profiles should be different.

Since the comparison between both MARSIS operational modes (AIS and subsurface) cannot be direct because AIS does not provide any information of the bottomside, it was decided to use an empirical model to describe the bottomside. An empirical model was chosen instead of a photochemical or a numerical one because this kind of model is based on the behavior of real data. Although there is a potential uncertainty in this approach which is introduced by the uncertainty in the bottomside profile, we consider that this is the closest approach to reality.

A clear outcome of this work is the need for investigating the sources of discrepancies between the various data sets. It is important to consider that the uncertainty of each TEC processing technique could be a key point to mention. Up to now, this parameter has not been reported for the MARSIS data acquired in the subsurface mode, although *Mouginot et al.* [2008] reported that the TEC derivation sensitivity at day and at night depends on the operational frequency of MARSIS and is about $3.8 \cdot 10^{14}$ and $1.5 \cdot 10^{14}\,\mathrm{m}^{-2}$, respectively (0.038 and 0.015 TECu, respectively). This TEC sensitivity is based on the signal power loss of 1 dB compared to the best correction used in their method. However, one can look at uncertainties estimated on analogous measures at Earth. This technique has been widely used in the study of the global vertical TEC in the Earth's ionosphere from altimetry missions such as TOPEX/Poseidon (1992–2005), JASON-1 (2001–2013),

JASON-2 (2008 until now), or JASON-3 (planned for launch in 2015) during the last two consecutive solar cycles. These missions were designed for accurate measurements of sea surface height, which requires the removal of the ionospheric delay imposed on the altimeter, resulting in TEC measurements between the sea surface and the satellite orbit altitude as a by-product of the satellite mission [*Fu et al.*, 1994; *Codrescu et al.*, 1999]. Therefore, the physics involved in the TEC retrieval is exactly the same as in the case of MARSIS, with the exceptions that on Earth, the frequencies used are much higher (e.g., 13.6 GHz for TOPEX) and that the amount of ionization on Earth can be up to 2 orders of magnitude higher. As in the case of both retrieval techniques of MARSIS studied in this paper, TOPEX and JASON's satellites should give similar results for TEC. The general conclusion is that TOPEX and JASON-1 are almost identical [*Yasyukevich et al.*, 2010] at least to within ±5 TECu (or within 10%), which is not statistically very meaningful in the case of Earth [*Jee et al.*, 2014]. Also, *Ping et al.* [2004], in the validation of JASON-1 by comparison of these data with global ionosphere maps from GPS data and with the empirical model International Reference Ionosphere (IRI) [*Bilitza*, 2001] for the first 2 years of JASON-1, concluded that the bias could be systematic at about 1.4 TECu, which is again statistically insignificant. Therefore, in our case after extrapolation to Mars, can the differences between the two subsurface retrieval techniques be considered statistically insignificant?

Regarding the Active Ionospheric Sounding Mode, the basic unit is the MARSIS ionogram, which consists of an array of received power plotted as a function of the sampled sounding frequencies and delay times. Following the routine inversion explained at, e.g., *Sánchez-Cano et al.* [2012] or *Morgan et al.* [2013], a topside vertical electron density profile is retrieved once the MARSIS ionogram has processed. The uncertainty in the local plasma frequency is typically 3% or less, while the uncertainty in altitude is 6.9 km, which is approximately 10% of the ionospheric peak altitude [*Morgan et al.*, 2008, 2013]. In addition, the manual or automatic scaling of the ionograms could lead to an additional error of about 10%. Moreover, other kinds of errors can be included in AIS and subsurface MARSIS data processing due to their own technique characteristics: since subsurface works better on the nightside because the carrier frequencies are much higher than the plasma frequency, the degree of reliability in the dayside has to be lower because the MARSIS frequencies are very close to the maximum plasma frequency. On the other hand, the AIS mode is very accurate on the dayside as this mode was specially designed for this end. Therefore, the best comparison between the two MARSIS modes is at the terminator, and indeed, this is where the best agreement is found.

In addition, we must take into account the following assumptions. First, the low-limit plasma detection by MARSIS in the AIS mode is as low as $1.24 \cdot 10^8\,\mathrm{m}^{-3}$ (corresponding to a plasma frequency of 0.1 MHz) [*Gurnett et al.*, 2008]. Second, a good local plasma density determination at the spacecraft altitude is essential for the electron density profile acquisition. Consequently, a good method of identification of the local plasma frequency is a key factor [*Andrews et al.*, 2013]. Third, this study has been based on the assumption that all the analyzed TEC (from both modes) is due to the ionosphere underneath the spacecraft. However, the MARSIS measurements are usually taken between 1200 km and 275 km (orbit pericenter). This means that when the spacecraft is at the pericenter, the ionospheric plasma under the spacecraft corresponds to the 95–98% of the total. Therefore, there is 2–5% of the ionosphere above the spacecraft that it is not analyzed either in subsurface or AIS operational modes. On the contrary, the TEC from NeMars model is calculated for a constant altitude interval of 50–400 km.

5. Conclusions

Due to the usefulness that the total electron content has in ionospheric characterization and monitoring, it is important to understand the available data sets. Following a critical assessment of those estimates with the MARSIS instrument, we can conclude that

1. Data from the nightside and terminator, $\chi > 75°$, regions can be confidently used since the differences among all data sets are less than 0.2 TECu.
2. On the dayside, $\chi < 75°$, we recommend caution with the use of the subsurface data values. The differences between both subsurface algorithms on the dayside can be up to 1 TECu around 60° solar zenith angle and by 0.3 TECu in average. At least, an error bar between 0.3 and 1 TECu should be considered. The method from Mouginot et al. gives the same value as the topside sounder which could be explained only with a fast-decaying ionization layer below the main peak. The method from Cartacci et al. seems to be more consistent with topside sounder at the smaller solar zenith angles.

In order to fully address the issue shown in this paper, it is recommended that future analyses include (1) further comparisons with the SHARAD radar data aboard Mars Reconnaissance Orbiter [*Campbell et al.*, 2014], (2) additional comparisons with Mars Express radio occultation data [*Peter et al.*, 2014], (3) numerical simulations of the radar wave propagation, and (4) testing of the retrieval technique stability and sensitivity.

Acknowledgments

B.S.-C. and M.L. acknowledge support through STFC grant ST/K001000/1. Also, B.S.-C. acknowledges the Spanish project AYA2011-29967-C05-02, the Complutense Predoctoral Fellowship that she had until 17 June 2014 and two scientific stays at ESTEC of the European Space Agency by ESTEC Faculty support funding. D.M. was supported at The University of Iowa under contract 1224107 with the Jet Propulsion Laboratory. The Mars Express MARSIS AIS raw data and the first years of MARSIS subsurface data [*Mouginot et al.*, 2008] were downloaded from the European Space Agency Planetary Science Archive (http://www.rssd.esa.int/psa). The rest of MARSIS subsurface data can be requested either to the authors of this manuscript or to the authors of *Mouginot et al.* [2008] and *Cartacci et al.* [2013]. The NeMars data are the results of the empirical model described at *Sánchez-Cano et al.* [2013]. All data will be available on request to the author (bscmdr1@leicester.ac.uk). The authors thank the Mars Upper Atmosphere Network (MUAN) led by H. Opgenoorth for fruitful discussions at their semiannual meetings.

Michael Liemohn thanks the reviewers for their assistance in evaluating this paper.

References

Aarons, J., M. Mendillo, and R. Yantosca (1996), GPS phase fluctuations in the equatorial region during the MISETA 1994 campaign, *J. Geophys. Res.*, *101*(A12), 26,851–26,862, doi:10.1029/96JA00981.

Andrews, D. J., H. J. Opgenoorth, J. T. Edberg, M. Andre, M. Franz, E. Dubinin, F. Duru, D. Morgan, and O. Witasse (2013), Determination of local plasma densities with the MARSIS radar: Asymmetries in the high-altitude Martian ionosphere, *J. Geophys. Res. Space Physics*, *118*, 6228–6242, doi:10.1002/jgra.50593.

Bilitza, D. (2001), International Reference Ionosphere 2000, *Radio Sci.*, *36*(2), 261–275, doi:10.1029/2000RS002432.

Budden, K. G. (1985), *The Propagation of Radio Waves*, Cambridge Univ. Press, Cambridge, U. K.

Campbell, B. A., N. E. Putzig, F. J. Foss, and R. J. Phillips (2014), SHARAD signal attenuation and delay offsets due to the Martian ionosphere, *IEEE Geosci. Remote Sens. Lett.*, *11*(3), doi:10.1109/LGRS.2013.2273396.

Cartacci, M., E. Amata, A. Cicchetti, R. Noschese, S. Giuppi, B. Langlais, A. Frigeri, R. Orosei, and G. Picardi (2013), Mars ionosphere total electron content analysis from MARSIS subsurface data, *Icarus*, *223*(1), 423–437, doi:10.1016/j.icarus.2012.12.011.

Chicarro, A., P. Martin, and R. Traunter (2004), Mars Express: A European mission to the red planet, European Space Agency Publication Division, SP-1240, pp. 3–16, Noordwijk, Netherlands.

Codrescu, M. V., S. E. Palo, X. Zhang, T. J. Fuller-Rowell, and C. Poppe (1999), TEC climatology derived from TOPEX/Poseidon measurements, *J. Atmos. Sol. Terr. Phys.*, *61*, 281–298.

Fox, J. L. (2009), Morphology of the dayside ionosphere of Mars: Implications for ion outflows, *J. Geophys. Res.*, *114*, E12005, doi:10.1029/2009JE003432.

Fu, L. L., E. J. Christensen, C. A. Yamarone, M. Lefbvre, Y. Menard, M. Dorrer, and P. Escudier (1994), TOPEX/Poseidon mission overview, *J. Geophys. Res.*, *99*, 24,369–24,381, doi:10.1029/94JC01761.

Gurnett, D. A., et al. (2005), Radar soundings of the ionosphere of Mars, *Science*, *310*, 1929–1933, doi:10.1126/science.1121868.

Gurnett, D. A., et al. (2008), An overview of radar soundings of the Martian ionosphere from the Mars Express spacecraft, *Adv. Space Res.*, *41*, 1335–1346, doi:10.1016/j.asr.2007.01.062.

Hargreaves, J. K. (1992), *The Solar-Terrestrial Environment*, 218 pp., Cambridge Univ. Press, Cambridge, U. K.

Jakowski, N., S. Heise, A. Wehrenpfennig, and S. Schliiter (2001), TEC monitoring by GPS: A possible contribution to space weather monitoring, *Phys. Chem. Earth*, *26*(8), 609–613.

Jee, G., H.-B. Lee, and S. C. Solomon (2014), Global ionospheric total electron contents (TECs) during the last two solar minimum periods, *J. Geophys. Res. Space Physics*, *119*, 2090–2100, doi:10.1002/2013JA019407.

Kintner, P. M., and B. M. Ledvina (2005), The ionosphere, radio navigation, and global navigation satellite systems, *Adv. Space Res.*, *35*, 788–811, doi:10.1016/j.asr.2004.12.076.

Klobuchar, A., and J. Aarons (1973), Importance of the total electron content parameter, in *Total Electron Content Studies of the Ionosphere*, Air Force Survey in Geophysics, no. 257, Bedford, Mass.

Leitinger, R., N. Jakowski, K. Davies, G. K. Hartmann, and E. Feichter (2000), Ionospheric electron content and space weather: Some examples, *Phys. Chem. Earth*, *25*(8), 629–634.

Lillis, R. J., D. A. Brain, S. L. England, P. Withers, M. O. Fillingim, and A. Safaeinili (2010), Total electron content in the Mars ionosphere: Temporal studies and dependence on solar EUV flux, *J. Geophys. Res.*, *115*, A11314, doi:10.1029/2010JA015698.

Mendillo, M., A. Lollo, P. Withers, M. Matta, M. Pätzold, and S. Tellmann (2011), Modeling Mars' ionosphere with constraints from same-day observations by Mars Global Surveyor and Mars Express, *J. Geophys. Res.*, *116*, A11303, doi:10.1029/2011JA016865.

Mendillo, M., C. Narvaez, P. Withers, M. Matta, W. Kofman, and J. Mouginot (2013), Variability in ionospheric total electron content at Mars, *Planet. Space Sci.*, *86*, 117–129, doi:10.1016/j.pss.2013.08.010.

Mitchell, C. N., L. Alfonsi, G. De Franceschi, M. Lester, V. Romano and A. W. Wernik (2005), GPS TEC and scintillation measurements from the polar ionosphere during the October 2003 storm, *Geophys. Res. Lett.*, *32*, L12S03, doi:10.1029/2004GL021644.

Morgan, D. D., D. A. Gurnett, D. L. Kirchner, J. L. Fox, E. Nielsen, J. J. Plaut (2008), Variation of the Martian ionospheric electron density from Mars Express radar soundings, *J. Geophys. Res.*, *113*, A09303, doi:10.1029/2008JA013313.

Morgan, D. D., O. Witasse, E. Nielsen, D. A. Gurnett, F. Duru, and D. L. Kirchner (2013), The processing of electron density profiles from the Mars Express MARSIS topside sounder, *Radio Sci.*, *48*, 197–207, doi:10.1002/rds.20023.

Mouginot, J., W. Kofman, A. Safaeinili, and A. Herique (2008), Correction of the ionospheric distortion on the MARSIS surface sounding echoes, *Planet. Space Sci.*, *56*, 917–926, doi:10.1016/j.pss.2008.01.010.

Němec, F., D. D. Morgan, D. A. Gurnett, F. Duru, and V. Truhlík (2011), Dayside ionosphere of Mars: Empirical model based on data from the MARSIS instrument, *J. Geophys. Res.*, *116*, E07003, doi:10.1029/2010JE003789.

Peter, K., et al. (2014), The dayside ionospheres of Mars and Venus: Comparing a one-dimensional photochemical model with MaRS (Mars Express) and VeRa (Venus Express) observations, *Icarus*, *233*, 66–82, doi:10.1016/j.icarus.2014.01.028.

Pi, X., A. J. Mannucci, U. J. Lindqwister, and C. M. Ho (1997), Monitoring of global ionospheric irregularities using the worldwide GPS network, *Geophys. Res. Lett.*, *24*(18), 2283–2286, doi:10.1029/97GL02273.

Picardi, G., and S. Sorge (2000), Adaptive compensation of ionosphere dispersion to improve subsurface detection capabilities in low-frequency radar systems, Proc. SPIE, Eighth International Conference on Ground Penetrating Radar, vol. 4084, pp. 624–629.

Picardi, G., et al. (2004), Mars Express: A European mission to the red planet, MARSIS: Mars Advanced Radar for Subsurface and Ionosphere Sounding, European Space Agency Publication Division, SP-1240, pp. 51–70, Noordwijk, Netherlands.

Picardi, G., et al. (2008), Mars ionosphere data inversion by MARSIS surface and subsurface signal analysis, IEEE RADAR CONFERENCE, VOLS. 1–4 Collection: IEEE Radar Conference, pp. 1278–1282.

Ping, J., K. Matsumoto, K. Heki, A. Saito, P. Callahan, L. Potts, and C. H. Shum (2004), Validation of Jason-1 nadir ionosphere TEC using GEONET, *Mar. Geod.*, *27*, 741–752, doi:10.1080/01490410490889049.

Rees, M. H. (1989), *Physics and Chemistry of the Upper Atmosphere*, 98 pp., Cambridge Univ. Press, Cambridge, U. K.

Safaeinili, A., W. Kofman, J.-F. Nouvel, A. Herique, and R. L. Jordan (2003), Impact of Mars ionosphere on orbital radar sounder operation and data processing, *Planet. Space Sci.*, *51*, 505–515, doi:10.1016/S0032-0633(03)00048-5.

Safaeinili, A., W. Kofman, J. Mouginot, Y. Gim, A. Herique, A. B. Ivanov, J. Plaut and G. Picardi (2007), Estimation of the total electron content of the Martian ionosphere using radar sounder surface echoes, *Geophys. Res. Lett.*, *34*, L23204, doi:10.1029/2007GL032154.

Sánchez-Cano, B., O. Witasse, M. Herraiz, S. M. Radicella, J. Bauer, P.-L. Blelly, and G. Rodríguez-Caderot (2012), Retrieval of ionospheric profiles from the Mars Express MARSIS experiment data and comparison with radio occultation data, *Geosci. Instrum. Methods Data Syst.*, *1*, 77–84, doi:10.5194/gi-1-77-2012.

Sánchez-Cano, B., S. M. Radicella, M. Herraiz, O. Witasse, and G. Rodríguez-Caderot (2013), NeMars: An empirical model of the Martian dayside ionosphere based on Mars Express MARSIS data, *Icarus*, *225*, 236–247, doi:10.1016/j.icarus.2013.03.021.

Seu, R., et al. (2007), The SHARAD sounding radar on MRO, *J. Geophys. Res.*, *112*, E05S05, doi:10.1029/2006JE002475.

Withers, P., et al. (2012), A clear view of the multifaceted dayside ionosphere of Mars, *Geophys. Res. Lett.*, *39*, L18202, doi:10.1029/2012GL053193.

Yasyukevich, Y. V., E. L. Afraimovich, K. S. Palamartchouk, and P. V. Tatarinov (2010), Cross testing of ionosphere models IRI-2001 and IRI-2007, data from satellite altimeters (TOPEX/Poseidon and Jason-1) and global ionosphere maps, *Adv. Space Res.*, *46*, 990–1007, doi:10.1016/j.asr.2010.06.010.